Magnetic characterization using a three-dimensional hysteresis projection, illustrated with a study of limestones

Graham J. Borradaile, France Lagroix

Geophys. J. Int. (2000) **141,** 213–226

Magnetic characterization using a three-dimensional hysteresis projection, illustrated with a study of limestones

Graham J. Borradaile and France Lagroix

Department of Geology, Lakehead University, Thunder Bay, Ontario P7B 5E1, *Canada. E-mail: borradaile@lakeheadu.ca*

Accepted 1999 November 10. Received 1999 November 1; in original form 1999 July 30

SUMMARY

Limestones provide an important source of palaeomagnetic information despite their low content of submicroscopic remanence-bearing minerals. The chief sources of these minerals are thought to be clastic volcanic magnetite and titanomagnetite, and organic magnetite, the latter mostly from bacterial sources. Chemically remagnetized limestones carry magnetite or pyrrhotite. Three hysteresis properties prove useful in identifying and characterizing these mineralogical influences on limestones: the ratio of zero-field maximum remanence to saturation remanence (M_r/M_s) in an applied field, coercivity of remanence (B_{cr}) and coercivity (B_c). To a lesser extent K_f/M_s may be useful, where K_f is the ferrimagnetic susceptibility. Traditionally, these have been plotted on a combination of 2-D graphs that of necessity only preserve two variables (Day *et al.* 1977; Wasilewski 1973). However, we found that magnetic discrimination and characterization of the limestones was much easier on a three-axis hysteresis projection that preserves the values of B_{cr}, B_c and M_r/M_s as independent variables. Using logarithmic scales, the regression surfaces through the data become almost planar and distinguish pelagic, shallow marine, shelf and remagnetized limestones on the basis of the slope and intercept of the associated regression surface. Clearly, there are sensitive sedimentological, geochemical or organic influences that dictate the magnetic mineralogy through sedimentary environment. Moreover, the 3-D plot of hysteresis criteria affords easy recognition of remagnetized limestones and may permit the rejection of material unsuitable for palaeomagnetic study. The 3-D hysteresis projection may be useful for the characterization of other rocks and magnetic materials

Key words: chemical remagnetization, limestones, magnetic hysteresis, magnetic materials.

INTRODUCTION

Despite their weak remanence, often $<10\,\mathrm{mA\,m^{-1}}$, much valuable palaeomagnetic information is now obtained from limestones, and this has sparked interest in the rock magnetic properties that influence and characterize their magnetic behaviour (Lowrie & Heller 1982; Freeman 1986). Previously, it has been shown that the hysteresis parameters differ from one sedimentary environment to another (Borradaile *et al.* 1993). Since there are a limited number of different possible sources of remanence-bearing minerals, it seems reasonable to hypothesize that the few distinctive marine depositional environments should control the proportions of magnetic grains and be characterized by their magnetic properties.

Briefly, the main *primary* origins of remanence-carrying minerals in limestones fall into two classes: physical and biogenic. The physical sources may be *clastic*, *exhalative*, *extraterrestrial* or *chemical-authigenic*. Clastic titanomagnetite, usually characterized by traces of Cr, is attributed to subaerial dust from continental, island arc or submarine environments (Henshaw & Merrill 1980; Freeman 1986); however, magnetite inclusions carried by fluvial clay minerals of continental origin may be dispersed to great distances in the oceans. Exhalative iron oxides associated with mid-ocean ridge emissions may cover large areas, for example of the North Pacific, and are chiefly of haematite. Cosmic magnetite spherules, commonly with traces of Ni, are ubiquitous and could be a significant source of remanence in slowly accumulating sediments that are isolated from continental detritus. Chemical authigenic processes are poorly understood but should also be considered as possible sources of iron oxides in marine environments, as emphasized by Mackereth (1971) and Henshaw & Merrill (1980). However, Chang & Kirschvink (1989) caution that the physical conditions required are rarely encountered in nature.

The relative roles of these physical sources of iron oxides will vary with depositional and chemical environment, but the consensus seems to be that clastic volcanic sources, chiefly providing magnetite and titanomagnetite, should be significant.

There are well known sources of biogenic remanence; all are due to magnetite and they include chiton teeth (Lowenstam 1962) and magnetite-producing bacteria (Blakemore 1975; Kirschvink & Lowenstam 1979; Kirschvink 1982). They are particularly important since all produce magnetite in grain sizes favourable to the preservation of durable palaeomagnetic signals. Chitons are magnetofossils with restricted stratigraphic range and palaeoenvironment, whereas the many species of magnetite-producing bacteria have been active since the early Proterozoic (~ 2 Ga) in a wider range of marine and fresh-water environments (Chang & Kirschvink 1989)—perhaps even on Mars (Kirschvink *et al.* 1997).

Magnetite-producing bacteria fall into two classes: magnetotactic bacteria and dissimilatory iron-reducing bacteria. The former grow intracellular single-domain magnetite arranged in chains for the purpose of short-range navigation (Frankel *et al.* 1981). The fossil preservation of this delicate linear magnetosome arrangement, producing characteristic magnetic interactions, may be quite fortuitous. In anoxic environments, iron-reducing bacteria are much more productive, shedding magnetite through their life cycle. Their more copious production is in a wide range of grain sizes from superparamagnetic (SP) to small pseudo-single domain (Moskowitz *et al.* 1989). Using rock-magnetic tests, Moskowitz *et al.* (1989) could distinguish them from linear magnetosomes of magnetotactic bacteria. However, their study involved bacterial cultures in the laboratory, in which interacting grains of magnetotactic chains were perfectly preserved.

Secondary remanence carriers are common in certain limestones. Lowrie & Heller (1982) note that acquisition of IRM or hysteresis studies in fields equivalent to values of <1 T may give a false impression of saturation and leave the researcher with the opinion that magnetite is the only carrier. Goethite, however, is a common contaminant. It may be of primary origin; indeed, it is the only iron oxide compatible with the Eh/pH conditions of seawater (Henshaw & Merrill 1980). One often suspects, however, a secondary origin that may be difficult to remove without destroying some useful part of the primary palaeomagnetic record. Haematite may also be a secondary mineral in limestones. A greater concern, albeit in restricted regions, is the extensive chemical remagnetization of limestones, involving the creation of new, fine-grained magnetite (Jackson 1990; Jackson & Sun 1992; McCabe & Channell 1994; Channell & McCabe 1994). Since its signal may have high unblocking temperatures, it may be difficult to recognize its secondary nature. Thus, these authors have developed numerous rock-magnetic criteria that identify chemically remagnetized limestones.

THE DATA

The use of the 3-D plot will be illustrated with our hysteresis data (Table 1), comprising 557 measurements of calcareous sediments from numerous published sources. The broad environmental categories, with numbers of measurements in parentheses, include pelagic chalks ($n=208$) and a pelagic-shallow transitional sequence ($n=99$) (Lagroix & Borradaile 2000); shallow water limestones ($n=42$) and shelf limestones ($n=76$), including some samples from Borradaile *et al.* (1993), Borradaile (1991, 1992, 1994, 1999) and Borradaile & Brann (1997) that were restudied. Remagnetized limestones include Jackson's (1990) data set ($n=21$), a larger set ($n=83$) from McCabe & Channell (1994), and a silicified shelf limestone ($n=28$) that differs from its unaltered counterpart (Maher *et al.* 2000). The latter is not 'remagnetized' in the sense of Jackson (1990), but our new 3-D hysteresis projection reveals some similarities. Using traditional 2-D projections as well as a new 3-D projection, we shall try to characterize these different limestone suites according to their environmental influences on rock-magnetic criteria.

In this study, we introduce a diagram used by Lagroix and Borradaile during a study of magnetic fabrics illustrating the neotectonic environment of Cyprus (Lagroix & Borradaile 2000). They showed that the wide variation in hysteresis properties did not hinder the use of anisotropy of remanence or low-field susceptibility for tectonic analysis. This paper focuses on the contribution of magnetite to the remanence and hysteresis of limestones from a wide range of locations and

Table 1. Mean and standard errors of hysteresis parameters.

Location	environment	n	B_{cr}	Std Err	B_c	Std Err	M_r/M_s	Std Err	K_f/M_s	Std Err
Various Locations-1	pelagic	24	40.8	3.2	9.3	0.9	0.141	0.014	–	–
Cyprus-1	pelagic	54	28.2	0.8	13.4	0.6	0.178	0.007	17.3	0.3
Israel	pelagic	30	66.2	7.6	10.2	1.1	0.122	0.011	–	–
England-1	pelagic	29	79.6	15.6	14.9	6.0	0.387	0.114	–	–
Italy	pelagic	71	33.5	0.6	14.4	0.2	0.228	0.009	–	–
Cyprus-2	shallow-pelagic	99	28.9	0.7	13.1	0.4	0.175	0.003	17.1	0.3
Various Locations-2	shallow	26	47.7	7.3	14.0	1.6	0.222	0.018	–	–
Cyprus-3	shallow	16	38.4	3.3	20.7	4.2	0.203	0.017	16.6	1.7
England-2	shelf	23	48.0	10.1	10.9	2.1	0.382	0.179	–	–
England-3	shelf	29	67.7	11.5	10.2	0.4	0.121	0.136	–	–
England-4	shelf (silicified)	28	39.8	1.4	21.5	1.4	0.173	0.007	–	–
England-5	shelf	24	79.4	19.1	12.7	3.3	0.150	0.035	–	–
Jackson (1990)	remagnetized-1	21	47.4	2.0	8.39	1.1	0.320	0.029	38.8*	3.6*
McCabe & Channell (1994)	remagnetized-2	83	46.0	0.8	7.8	0.4	0.216	0.009	–	–

B_{cr}, B_c are in units of mT (Jackson 1999); K_f/M_s in units of 10^{-6} m A^{-1} (or µm A^{-1}). * Data from table1 of Jackson *et al.* (1993)

Table 2. Linear regression data for Day plot parameters (Figs 3 and 4).

Location	Type	n	c intercept	b slope	R	test stat $\alpha=0.05$	signif.
Various Locations-1	pelagic	24	0.30	−0.58	0.53	2.93	√
Cyprus-1	pelagic	54	0.29	−0.57	0.73	7.70	√
Israel	pelagic	30	0.31	−0.54	0.61	4.07	√
England-1	pelagic	29	0.30	−0.57	0.40	2.27	√
Italy	pelagic	71	0.62	−1.26	0.75	9.42	√
Cyprus-1	shallow-pelagic	99	0.26	−0.58	0.53	6.16	√
Various Locations-2	shallow	26	0.28	−0.28	0.50	2.83	√
Cyprus-3	shallow	16	0.27	−0.48	0.73	4.00	√
England-2	shelf	23	0.71	−1.18	0.48	2.51	√
England-3	shelf	29	0.73	−1.42	0.70	5.09	√
England-4	shelf (silicified)	28	0.32	−0.98	0.85	8.23	√
England-5	shelf	24	0.66	−1.50	0.65	4.01	√
Jackson (1990)	remagnetized-1	21	0.90	−0.60	0.95	13.26	√
McCabe & Channell (1994)	remagnetized-2	83	0.82	−0.75	0.88	16.67	√

Regression was performed for the relationship $(M_r/M_s)=c(B_{cr}/B_c)^b$. The significance of the correlation is determined by comparing the test statistic, $R\sqrt{[(n-2)/(1-R^2)]}$, with t. Critical t-test values for a given sample size are listed in Table 3. Significant regressions at a 95 per cent confidence level are marked by $\sqrt{}$.

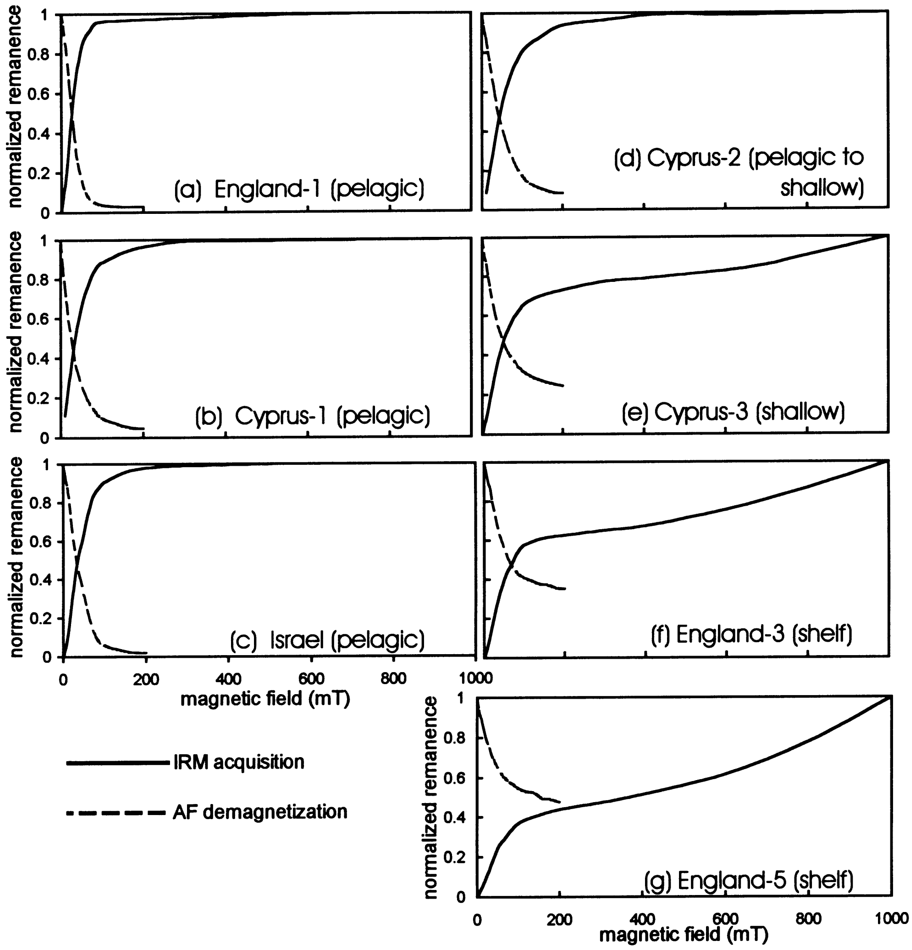

Figure 1. Cisowski (1981) showed that symmetrical IRM acquisition and subsequent AF demagnetization curves of the same sample, crossing at normalized intensities ~0.5 indicate the absence of magnetic interactions between magnetite grains. For our samples, the normalized intensity at the intersection is 0.45 ± 0.04 (std err.). Interacting SD grains would produce an assemblage more difficult to magnetize than demagnetize, so the intersection occurs at a normalized intensity ≪0.5. Following the cautionary advice of Lowrie & Heller (1982) we magnetized all samples to at least 1 T in both IRM acquisition and hysteresis studies to detect whether any of the common high-coercivity phases are present (e.g. goethite, maghemite). The failure of (e) (f) and (g) to saturate shows that they probably contain such a phase.

palaeoenvironments. The hysteresis parameters, coercivity B_c and coercivity of remanence B_{cr}, in units of millitesla (Jackson 1999), are important in distinguishing between single domain (SD), pseudo-single domain (PSD) and multidomain (MD) states in magnetite. The ratio M_r/M_s of zero-field (or low-field) remanence (M_r) to saturation remanence (M_s) is zero for superparamagnetic sizes but peaks for SD and small PSD sizes. Wasilewski (1973) plotted B_c versus B_{cr} to successfully distinguish SP/SD/PSD/MD states for magnetite, and Day *et al.* (1977) extended this by plotting (M_r/M_s) against (B_{cr}/B_c). Generally, judicious choice of one or both plots may prove effective in characterizing behaviour, or discriminating between rock-magnetic properties. This was the approach used, for example, by Borradaile *et al.* (1993). It is, however, useful to preserve the information contained in the individual coercivity values, rather than merging them as a ratio, B_{cr}/B_c. We will show subsequently that a 3-D plot of B_{cr} versus B_c versus M_r/M_s is more versatile in this regard and combines the best of the Wasilewski and Day *et al.* plots.

All our hysteresis data were obtained with an alternating field gradiometer, the Princeton Measurements Corporation MicroMag 2900, usually using a peak direct field of 1 T. Hysteresis loops were corrected for the diamagnetic or paramagnetic matrix contribution. Supplementary data on SIRM acquisition and AF demagnetization were derived with equipment supplied by Molspin and Sapphire Instruments.

DATA ANALYSIS

Table 1 summarizes the main hysteresis values determined for our limestone samples. Table 2 provides the information on regression surfaces that fit the hysteresis data distributions in a new 3-D projection (B_{cr}: B_c: M_r/M_s) described below. Table 4 lists regression data for the 3-D plots.

One of the simplest characterizations from hysteresis uses the ratio M_r/M_s. Low values indicate a superparamagnetic contribution, and peak values favour SD or PSD behaviour. In our context, the observations of Moskowitz *et al.* (1989) on the hysteresis of laboratory-cultured bacteria are important. For the magnetotactic bacteria, whose magnetosomes encapsulate a chain of small SD magnetite grains, typically they found $M_r/M_s \sim 0.41$. This value is within the range of error for only two of our sample suites (Table 1: pelagic, England-1; shelf, England-2), but this is not conclusive. Our samples are rocks in which magnetite chains could have been disrupted after organic decay, compaction, and, in the case of the Cyprus suite, mild tectonism. The interaction expected between the SD magnetite crystals of intact magnetosomes is not recognized in this study either: it is generally more difficult to magnetize than demagnetize all of our limestones, especially the shallow marine and shelf varieties (Fig. 1: method of Cisowski 1981). Cisowski showed that interactive SD grains are more difficult to magnetize than AF-demagnetize. Thus, their remanence-acquisition curves intersect the AF demagnetization curves at a normalized remanence value ~ 0.25. Non-interacting grains magnetize and demagnetize equally easily, producing symmetrical curves that intersect at normalized remanences ~ 0.5. For our data, the normalized remanences of acquisition–AF demagnetization curve intersections average 0.45 ± 0.04 (std err.), close to the ideal value of 0.5 for non-interacting grains (Fig. 2).

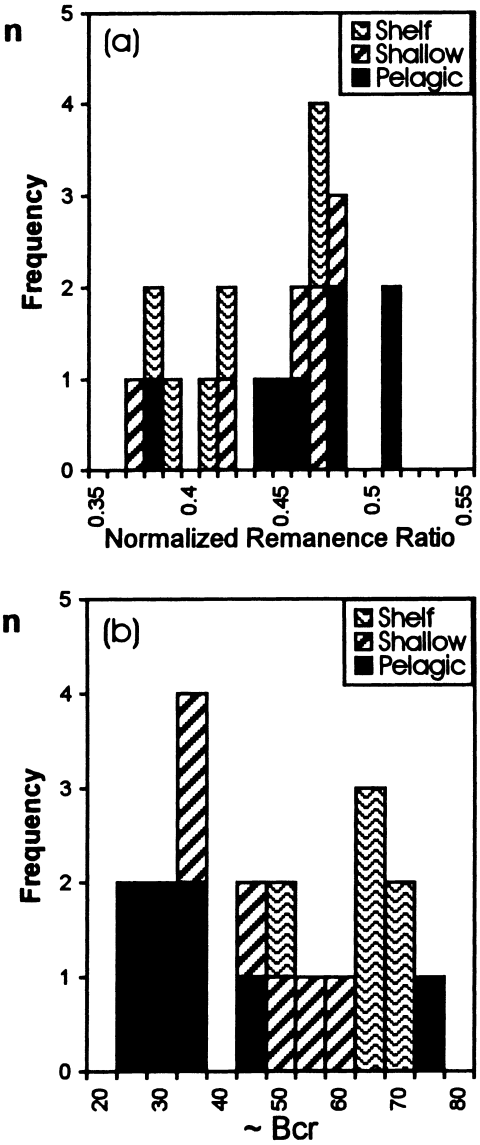

Figure 2. (a) Histograms showing the frequency distributions of the normalized magnetizations at which IRM acquisition and AF demagnetization curves intersect. None of our samples indicate the potential for magnetic interaction (intersections $\ll 0.5$), which is found for example in the closely juxtaposed magnetite grains of magnetotactic bacteria. (b) Frequency distributions of the coercivities of remanence (B_{cr}).

Another hysteresis ratio that provides characterization is the M_r/M_s intercept at $B_{cr} = B_c$. For example, $M_r/M_s \sim 0.86$ and ~ 0.82 have been reported from regionally remagnetized limestones (Jackson 1990; McCabe & Channell 1994, respectively). The chemical remagnetization is attributed to late or post-orogenic, anchimetamorphic fluid migration that triggered the formation of illite and chlorite, with fine-grained magnetite as a byproduct (Lu *et al.* 1991).

At $B_{cr} = B_c$ we recognize generally consistent values of $M_r/M_s \sim 0.3$ for pelagic chalks (Figs 3a to d), and $M_r/M_s \sim 0.7$ for shelf carbonates (Figs 3i, j, l). However, a silicified shelf limestone also has $M_r/M_s \sim 0.3$ (Fig. 3k). Shallow water limestones have slightly lower intercepts ~ 0.27 (Figs 3f to h). This seems to corroborate the use of this simple parameter to

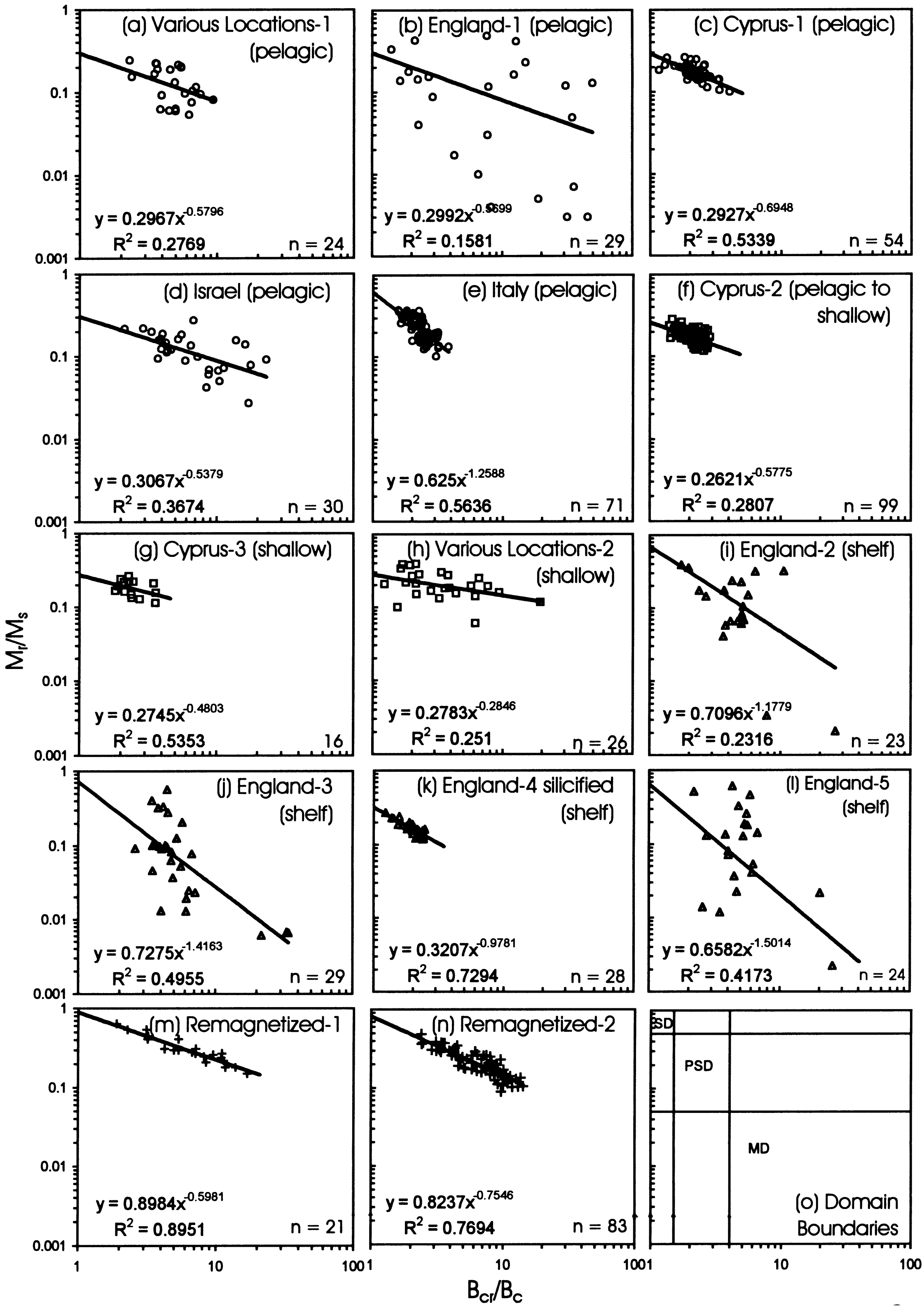

Figure 3. The conventional hysteresis plot of Day *et al.* (1977) indicating the distribution of our data and some from the literature. Regression lines significant at the 95 per cent level are shown. The high $M_r/M_s = 0.89$ considered to be indicative of remagnetization due to magnetite (Jackson 1990), or perhaps magnetite and pyrrhotite (Jackson *et al.* 1993) shown in (m) is not recognized in any other suites we studied. Critical values associated with bacterial magnetite are not recognized either. It will be shown that these suites can be differentiated on hysteresis parameters in a three-axis plot below.

discriminate between sedimentary environments on the basis of magnetic mineralogy.

The recognition of remagnetization in limestones is important for palaeomagnetists, who naturally avoid secondary magnetizations in most aspects of palaeomagnetic and tectonic reconstructions. Channell & McCabe (1994) used the Day plot to discriminate successfully between two large data sets of remagnetized and non-remagnetized limestones, from Italy and England. They showed that data for remagnetized limestones followed a gentler slope than the SD-PSD-MD trend (compare Figs 3m and n with Fig. 3o). Essentially, the (B_{cr}/B_c) ratios were too high, due to the presence of secondary fine magnetite that also produced wasp-waisted hysteresis loops. Jackson *et al.* (1993) explain this as the result of a bimodal coercivity distribution: low-coercivity grains carry more M_s, and harder grains carry more M_r, thus displacing data to the right of the SD-PSD-MD trend on the Day plot (see, for example, our Figs 3m and n). For our data, the traditional Day plots reveal some interesting general trends with best fit lines in log–log space being shallowest for shallow-water limestones (Fig. 4b), steeper for pelagic limestones (Fig. 4a), and steepest for shelf limestones (Fig. 4c). Regression data for the Day Plots are in Table 2, with all regression lines significant at the 95 per cent level using the t-test, for which selected critical values are presented in Table 3.

We attempted to preserve the individual values B_{cr}, B_c by plotting these as x, y axes and then identifying these data points with contours of their associated M_r/M_s value. Thus all three pieces of hysteresis information could be combined on

Table 3. Critical values of t to be exceeded by the test statistic if $|R| > 0$. (A one-tailed test at the 95 per cent level).

$v = n - 2$	critical value	$v = n - 2$	critical value
5	2.571	30	2.042
10	2.228	40	2.021
15	2.131	60	2.000
20	2.086	120	1.980
25	2.060	∞	1.960

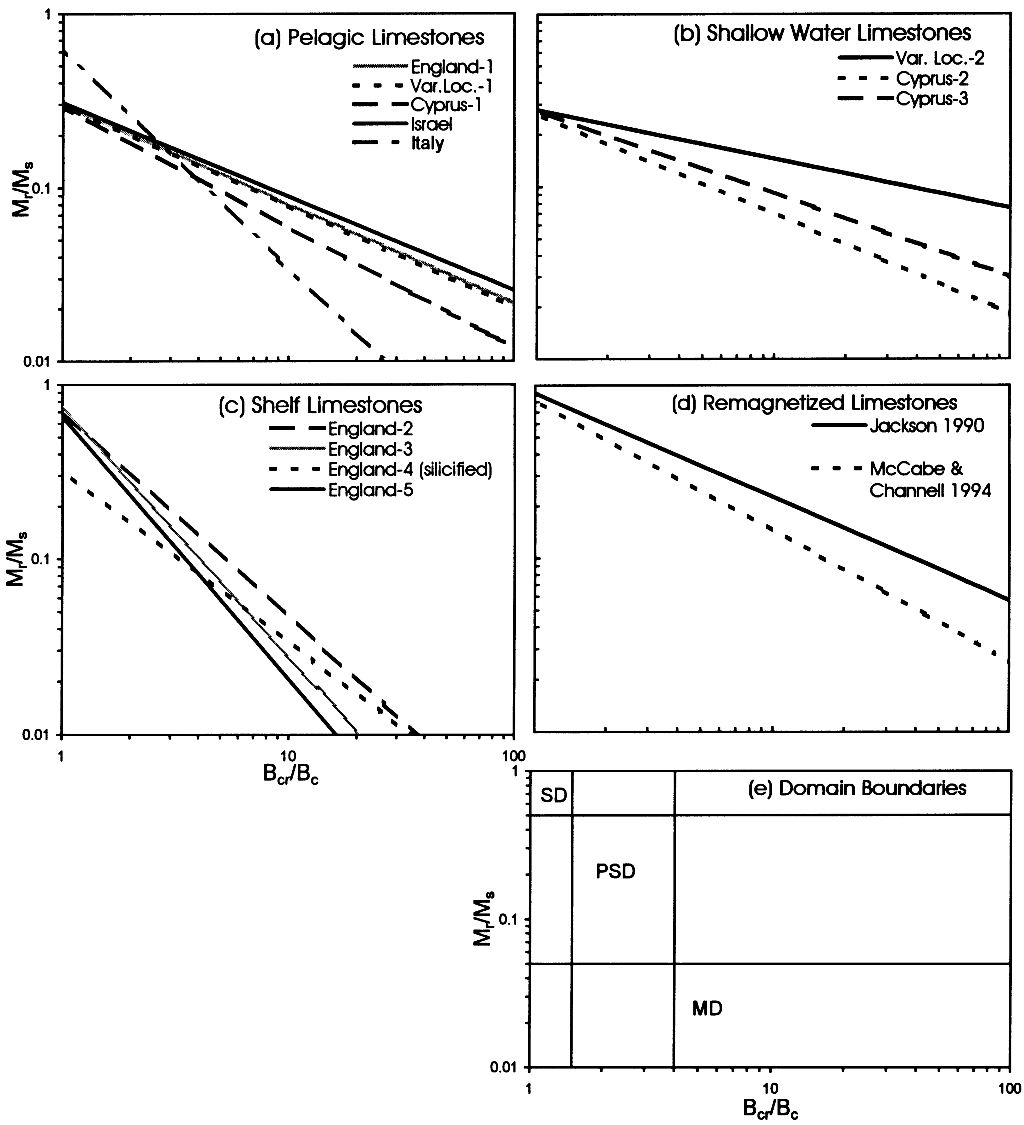

Figure 4. Summary and comparison of the Day plot regression lines significant at the 95 per cent level for the limestones studied.

one 2-D plot. Unfortunately, this is difficult to assess visually (Fig. 5). Thus, to preserve all the hysteresis measurements and exploit them to discriminate further among environments, we introduced the three-axis plots below.

3-D projection of data

The new projection preserves all measured parameters in one plot using logarithmic scales: $\log(B_{cr})$ versus $\log(B_c)$ versus $\log(M_r/M_s)$ $(x:y:z)$. We used the commercial software SIGMAPLOT v.5.0 to view the projection in any desired orientation. MD, PSD and SD responses occupy volumes represented by six-sided prisms (Fig. 6) whose bounds are defined by commonly accepted values (Dunlop & Özdemir 1997). Superparamagnetic (SP) responses should occupy the lowest level of the 3-D space plotted in Fig. 6, where $M_r/M_s \sim 0.01$. We chose an arbitrary orientation that shows clearly the main domain-response regimes in 3-D space, and, for the convenience of the reader, that can be used consistently with all our data in this paper. Other workers may choose equally valid alternative angles of view that are more suitable to their data, and which in SIGMAPLOT v.5.0 are interactively rotatable for enhanced visualization. Whereas traditional 2-D plots are cumbersome and obfuscate some trends, the 3-D projection clarifies patterns and reveals significant differences. This is aided by non-linear regression fitting the surface $\log(M_r/M_s)$ to $\log(B_{cr})$ and $\log(B_c)$ to define surfaces that generalize the behaviour of the sample suites. The t-statistic was used to determine where the correlation coefficients (R) were significantly non-zero at the 95 per cent level (using the critical values, examples of which are abbreviated in Table 3). Only significant results are graphed, for the relationship $\log(M_r/M_s) = a\log(B_{cr}) + b\log(B_c) + c$ (Table 4; Figs 7 to 10). By using logarithmic parameters, the regression surfaces become planar and thus are more readily visualized and distinguishable.

Hysteresis trends with depositional shallowing, illustrated by the 3-D plot

The Upper Cretaceous to Pliocene carbonate cover of Cyprus forms an upward shallowing sequence dated by micropalaeontology (Henson *et al.* 1949; Mantis 1970). It commences

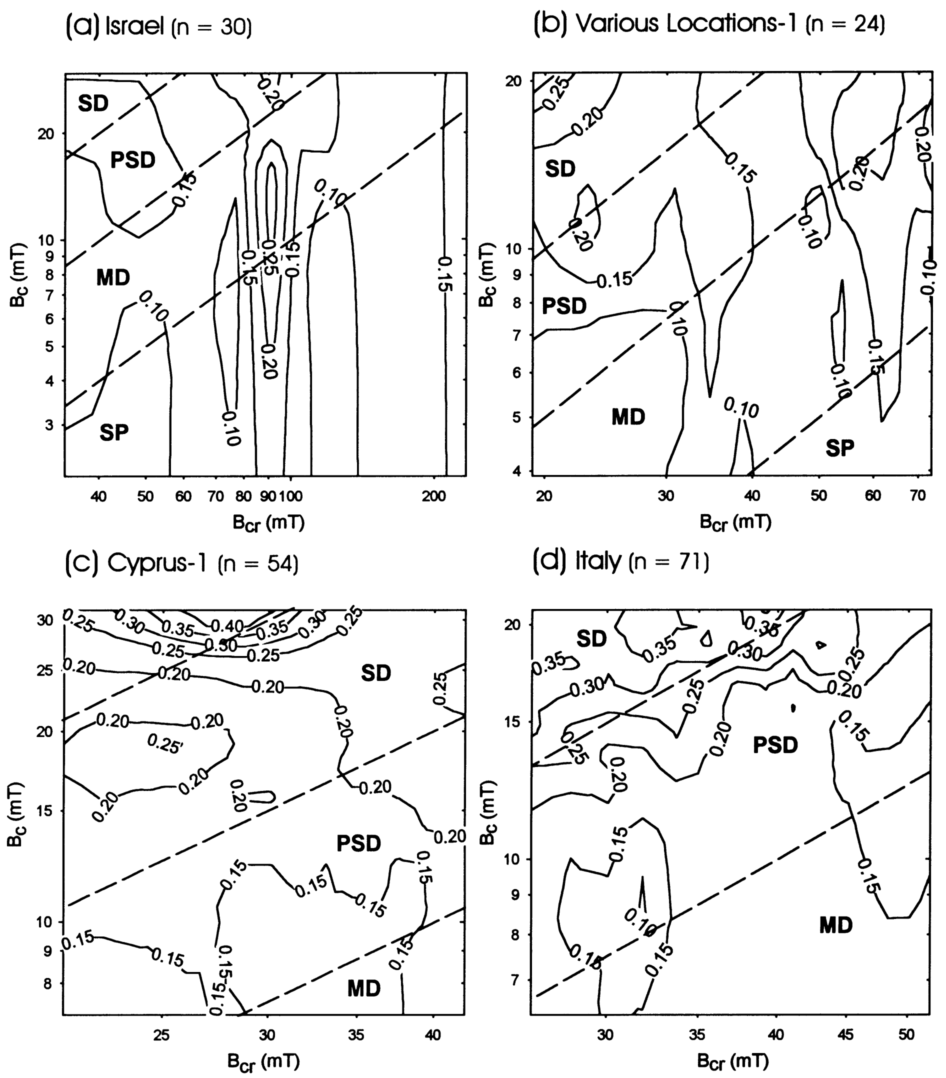

Figure 5. Plots of B_c versus B_{cr} with the data points of the pelagic limestone suites contoured according to their M_r/M_s ratio. Although this preserves all of the hysteresis parameters, this presentation is difficult to evaluate. Therefore, we developed the 3-D plot shown later.

Table 4. Planar regression data for 3-D log-hysteresis parameters (Figs 7 to 10).

Location	Type	n	a	b	c	R	test stat. $\alpha=0.05$	signif.
Various Locations-1	pelagic	24	n/s	0.013	n/s	0.76	5.48	√
Cyprus-1	pelagic	54	n/s	0.011	0.052	0.91	15.83	√
Israel	pelagic	30	n/s	0.008	0.055	0.72	5.49	√
England-1	pelagic	29	no significant regression plane					
Italy	pelagic	71	−0.005	0.026	n/s	0.80	11.08	√
Cyprus-1	shallow-pelagic	99	n/s	0.008	0.081	0.88	18.25	√
Various Locations-2	shallow	26	0.042	0.009	0.138	0.71	4.94	√
Cyprus-3	shallow	16	n/s	0.004	0.104	0.90	7.73	√
England-2	shelf	23	no significant regression plane					
England-3	shelf	29	no significant regression plane					
England-4	shelf (silicified)	28	n/s	0.006	0.091	0.94	14.05	√
England-5	shelf	24	no significant regression plane					
Jackson (1990)	remagnetized-1	21	−0.003	0.022	0.284	0.94	12.01	√
McCabe & Channell (1994)	remagnetized-2	83	n/s	0.020	0.098	0.91	19.75	√

The planar regression surface is defined by $\log(M_r/M_s)=a\log(B_{cr})+b\log(B_c)+c$. The significance of the correlation is determined by comparing the test statistic, $R\sqrt{[(n-2)/(1-R^2)]}$, with t. Significant regressions at a 95 per cent confidence level are marked by $\sqrt{}$.

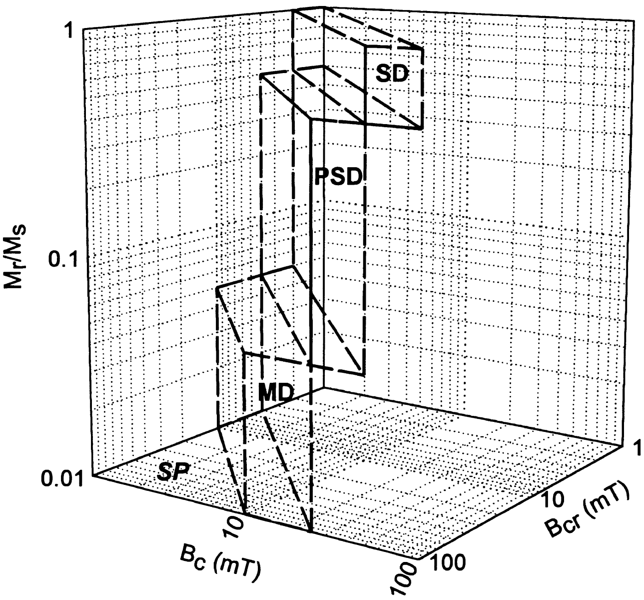

Figure 6. The three-axis hysteresis plot that facilitates the discrimination and comparison of the limestones that we studied. M_r/M_s is the ratio of zero-field maximum remanence to saturation remanence in an applied field. B_{cr} is the coercivity of remanence (mT), and B_c is the coercivity (mT). Superparamagnetic behaviour is described by conditions constrained to the basal plane in the triangular area indicated by SP. Multidomain (MD), pseudo-single domain (PSD) and single domain (SD) responses are described by parameters occupying the six-sided prismatic spaces indicated. The boundaries for the characteristic spaces are taken from Banerjee & Moskowitz (1985) and Dunlop & Özdemir (1997).

with the pelagic Lower Lefkara Formation, a 25-m thick chalk sequence of Maastrichtian age (74–65 Ma). The Middle Lefkara Formation is up to 300 m thick, a cherty sequence of Palaeocene to Eocene age (65–35 Ma). The Upper Lefkara Formation is a chalk sequence of middle to late Eocene age (35–23 Ma) that shows evidence of slumping and rapid uplift (Gass 1960). The overlying Pakhna Formation comprises shallow water carbonates with some reefs and gypsum of Miocene age (23–7 Ma) (Gass & Cockbain 1961; Mantis 1970). Finally, the uppermost Nicosia Formation includes marls and sandstones of early to middle Pliocene age (5–3 Ma). The Lefkara, Pakhna and Nicosia formations are, respectively, termed Cyprus-1, -2 and -3 in the tables. The data lie predominantly in the PSD field but the regression surfaces become progressively more gently dipping as the depositional environment becomes progressively shallower with time (Figs 7a to c). Such trends are, at the very least, difficult to observe by comparing different 2-D plots (e.g. Wasilewski 1973 versus Day *et al.* 1977) and are rather convoluted when using the contoured 2-D plot (Fig. 5) with which we experimented.

The 3-D plot clarifies trends: hysteresis regression planes slope more gently, as the depositional environment progresses from pelagic (Fig. 7a) to the shallowest depositional environment (Fig. 7c). The results are statistically significant and distinct (Tables 4 and 5), although one may debate the causes of the differences in magnetic mineralogy, in particular the relative roles of organic versus clastic magnetite, as the depositional depth changes.

Pelagic chalks

A comparison of carbonates with similar depositional environments from different areas is also instructive. Consider the pelagic chalks shown in Fig. 8, from Cyprus, Israel, Italy and England, *inter alia* (Jeans 1973; Borradaile 1994; Borradaile *et al.* 1993; Bernouilli & Jenkyns 1974). The data occupy PSD space clearly, trending towards MD. However, MD magnetite is virtually absent, and evidence for an SD response is completely

Table 5. Mean coercivity parameters for the upward shallowing carbonate sequence, Cyprus.

	B_c (mT)	M_r/M_s
shallow marine	20.71 ± 4.23	0.203 ± 0.017
pelagic	13.43 ± 0.56	0.178 ± 0.007

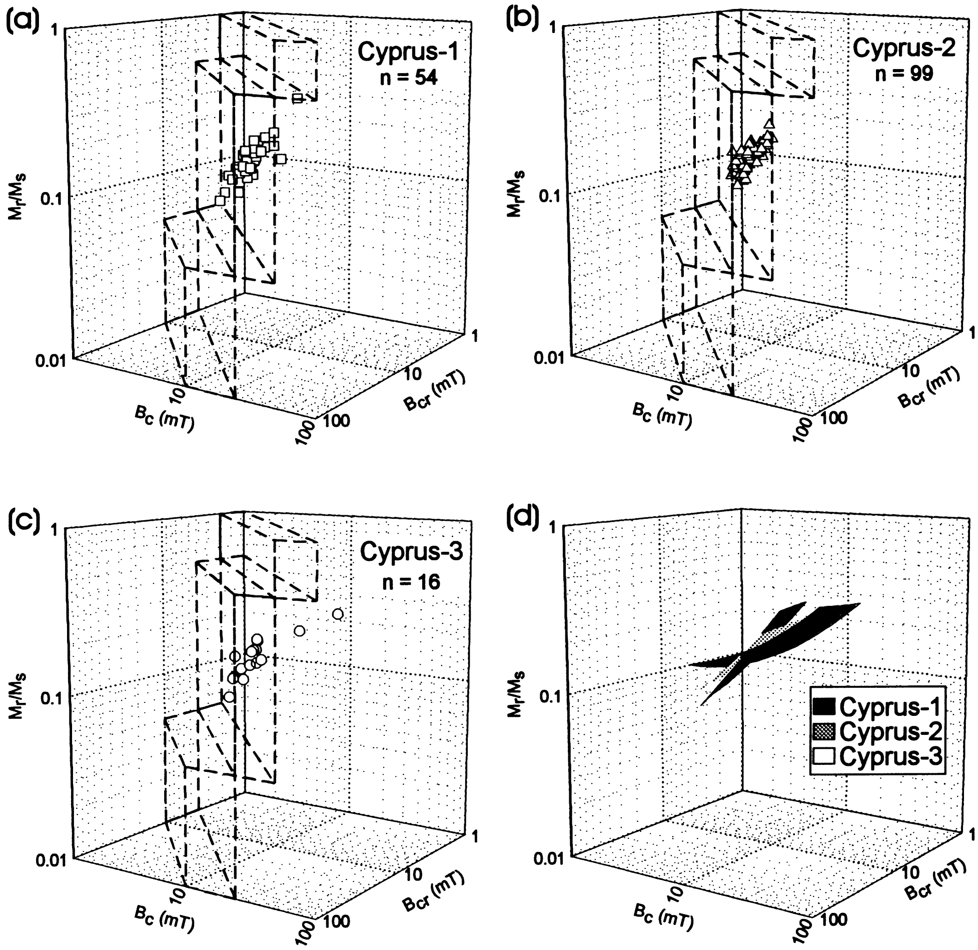

Figure 7. (a,b,c) An extensive continuous sequence of limestones in Cyprus was sampled, from pelagic types at the base (a) to progressively less deep depositional environments at the top (c). In the three-axis plot, the distribution of data is much clearer than in traditional 2-D Day plots (Fig. 3). (d) However, regression surfaces, significant at the 95 per cent level, still show more clearly the changing loci of hysteresis behaviour with depth of deposition. These surfaces appear nearly planar due to the logarithmic scaling of axes. This presumably indicates changing proportional influences of detrital input versus more homogeneous background sources of magnetite. In order of descending importance these are probably volcanic ash, bacterial sources or cosmic input. All occupy PSD space.

lacking in our samples. The regression surfaces are near-planar and similarly steep from widespread localities. [In contrast, shallow water limestones, from widespread localities, have gentler inclined regression surfaces (Fig. 9).] There is no conclusive indication of a bacterial component. The environment is, however, characterized by steep regression surfaces that more-or-less follow the locus of the SD-PSD-MD trend, for the most part clinging to or transgressing the low-B_c and high-B_{cr} boundaries of the PSD field. Of our samples, only the Israeli chalks include a few outliers in the MD field (Fig. 8a).

Shallow-water marine limestones

Generally located more centrally in the PSD field (Fig. 9), these data could be compatible with the grain sizes suspected where clastic input becomes more significant in littoral environments. The regression surfaces are significantly shallower than those for pelagic limestones (Fig. 8) and do not trend from SD towards MD but rather appear to transect the upper and lower B_c limits of the PSD field. The shallow regression surfaces are due to small variations in M_r/M_s and a restricted range of B_c values.

Remagnetized limestones

The data of Jackson (1990) provide hysteresis data for three limestone formations of Ordovician and Devonian age in the northeastern United States. These include the Trenton Limestone calcarenites and marls (Kay 1968), the Onondaga fine-grained and coralline limestone (Oliver 1960) and the Knox Dolomite, a fine-grained dolostone (Churnet *et al.* 1982). These were remagnetized in a pervasive fluid migration event that caused anchimetamorphic growth of magnetite associated with illite and chlorite (McCabe *et al.* 1984). Jackson noted that the data set yielded unusually high value of $M_r/M_s \sim 0.86$ at $B_{cr} = B_c$. Using the three-axis plot shown here we further recognize significant regression surfaces with inclinations slightly steeper than pelagic limestones but considerably steeper than for those of shallow-water and shelf limestones. However, the regression surfaces for remagnetized limestones are also displaced upwards above the locus of the SD-PSD-MD trend but with lower B_c values (Fig. 10e; Table 4). This re-enforces Jackson's (1990) observations of high M_r/M_s values using 2-D diagrams. The larger sample suite of remagnetized limestones from McCabe & Channell (1994), consisting of British

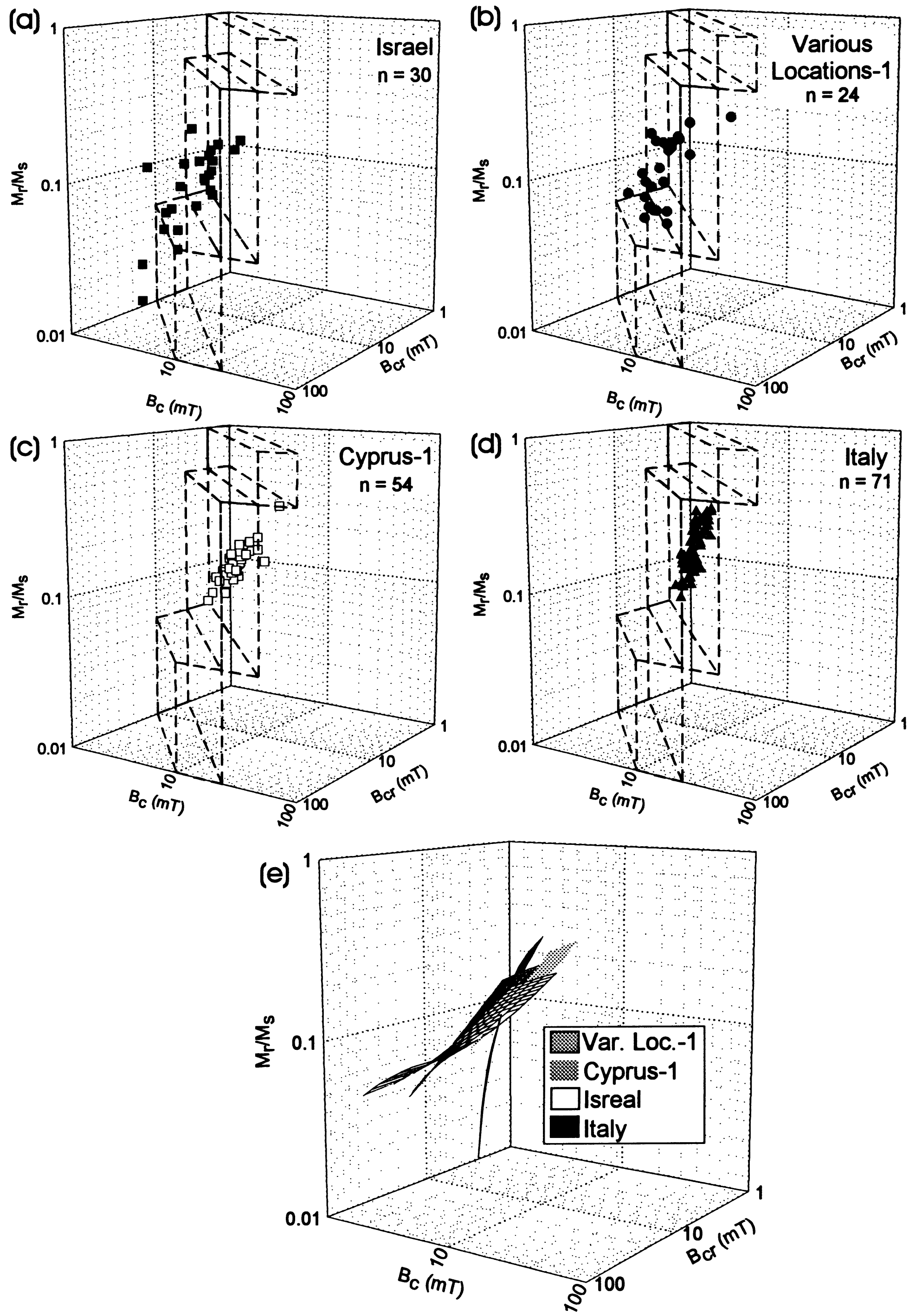

Figure 8. (a,b,c,d) Hysteresis parameters for pelagic limestones and chalks occupy steep surfaces in the 3-D plot in or close to PSD space, but generally near the low-B_c boundary. (e) The similarity of these environmental controls from widely differing locations is emphasized by the similarity of slopes of their regression surfaces, all significant at the 95 per cent level, and nearly planar in logarithmic scales.

Carboniferous Limestone (Earp *et al.* 1961) (Fig. 10d), has a similarly inclined regression plane in log–log space but a lower elevation (M_r/M_s intercept). Palaeomagnetists may be encouraged that remagnetized limestones may be more readily detected and rejected on the basis of the 3-D representation. Our sampling of shelf limestones from England included silicified examples. Although these are not remagnetized on the basis of any of the usual criteria, and they do not seem to have erased primary palaeomagnetic signals, the limestones did suffer a pervasive alteration. The silicified shelf limestones do, however, possess similarly inclined regression surfaces to those of the remagnetized limestones studied by Jackson and McCabe and Channell (Figs 10a and b), although their regression surfaces are displaced downwards; that is, they do not have the high M_r/M_s values recognized for true remagnetized limestone.

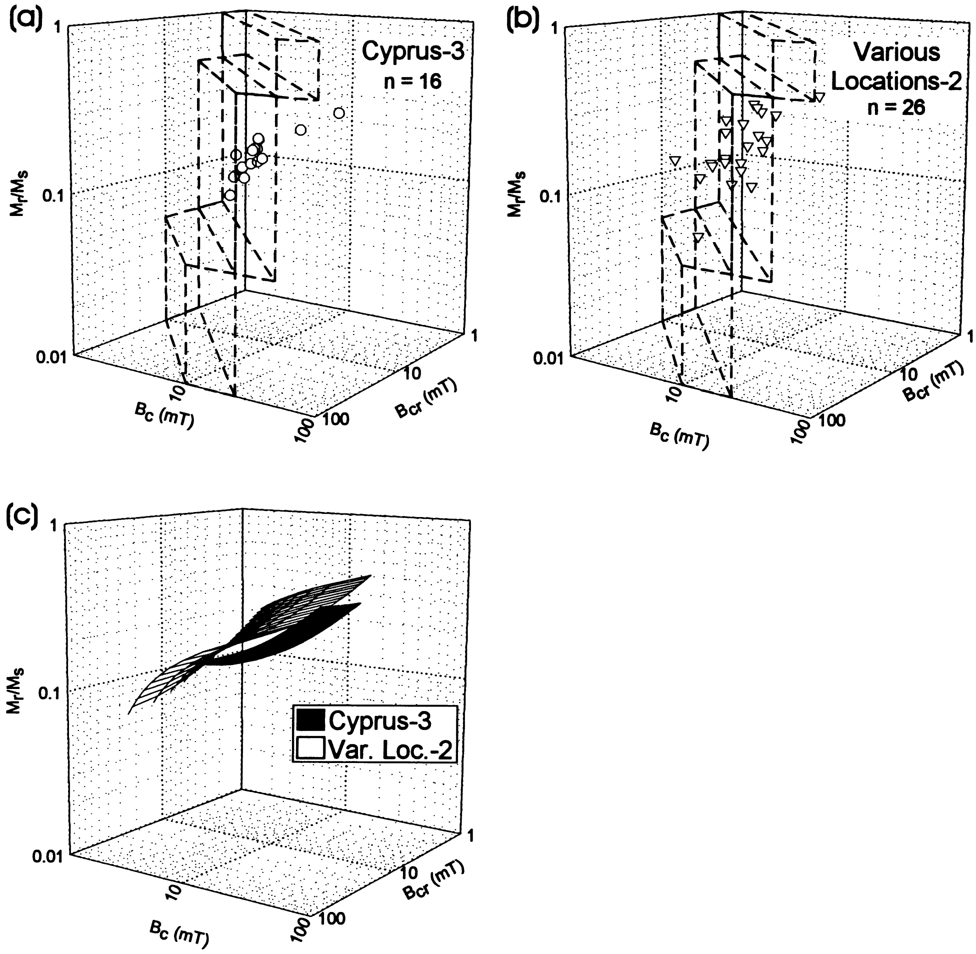

Figure 9. (a,b) Shallow marine limestones, from different locations around the world, show (c) gently inclined regression surfaces in PSD space but following a locus more gently inclined than the traditionally recognized SD-PSD-MD trend of zones.

Jackson *et al.* (1993) recognized the presence of pyrrhotite in previously studied remagnetized North American limestones. One of their conclusions is that high B_{cr}/B_c values may not always be interpreted in terms of bimodal magnetite grain-size/hysteresis distributions. They recognized that it may also be attributable to pyrrhotite, which they confirmed in the North American examples by recognizing its sharp reduction in remanence near 35 K.

The relationship $M_r/M_s \approx 0.89\ (B_{cr}/B_c)^{-0.6}$ is a convenient fingerprint for remagnetized limestone due to magnetocrystalline anisotropy of fine magnetite (Jackson 1990), although it need not be uniquely explained by magnetite, as Jackson *et al.* (1993) noted. The ratio K_f/M_s is an easily comprehended indication of fine-grained magnetite, for example due to chemical remagnetization, where K_f is the ferrimagnetic susceptibility. Values of $K_f/M_s \sim 80\ \mu m\ A^{-1}$ are common for the remagnetized samples studied by Jackson *et al.* (1993), $\sim 50\ \mu m\ A^{-1}$ for superparamagnetic grains, $\leq 35\ \mu m\ A^{-1}$ for bacterial magnetite (Moskowitz *et al.* 1988), and $\leq 8\ \mu m\ A^{-1}$ for stable single domain or larger grains. This criterion is presented for our most complete suite of limestones, in Cyprus, in Fig. 11. The ratio is essentially constant near 17.1 ± 0.2 (std err.), regardless of the depositional environment. This value does not rule out contributions from bacterial magnetite (reported as $\leq 8\ \mu m\ A^{-1}$), but is compatible with any small SD grains and a superparamagnetic contribution.

DISCUSSION

The presentation of hysteresis data in a three-axis plot preserves all three commonly measured hysteresis values, B_{cr}, B_c and M_r/M_s, and thus clarifies trends within the idealized SD-PSD-MD sequence, as well as indicating more clearly the anomalous trends lying outside this sequence. Non-linear regression in three dimensions identifies surfaces that characterize different sedimentary environments and remagnetized limestones in a visual manner. In logarithmic space these appear nearly planar, facilitating comparisons. The hysteresis parameters of pelagic limestones have steep regression surfaces, whereas those of shallow-water limestones are progressively less steep (Figs 7 to 9). Furthermore, shallow-water limestones have regression surfaces that do not follow the SD-PSD-MD trend but rather transgress the PSD field (Fig. 9). Remarkably, SD behaviour is absent from the limestone environments that we sampled, and MD magnetite is very rare. The hysteresis differences are primarily due to different effective magnetic grain sizes, although their geological origins are largely a matter of conjecture at the present. It seems difficult to characterize a bacterial source of magnetite with the routine hysteresis and rock-magnetic parameters we employed, including K_f/M_s.

A continuous carbonate sequence approximately 1 km thick in Cyprus shows a complete upward transition from pelagic chalks to shallow-water marine limestones. The change in

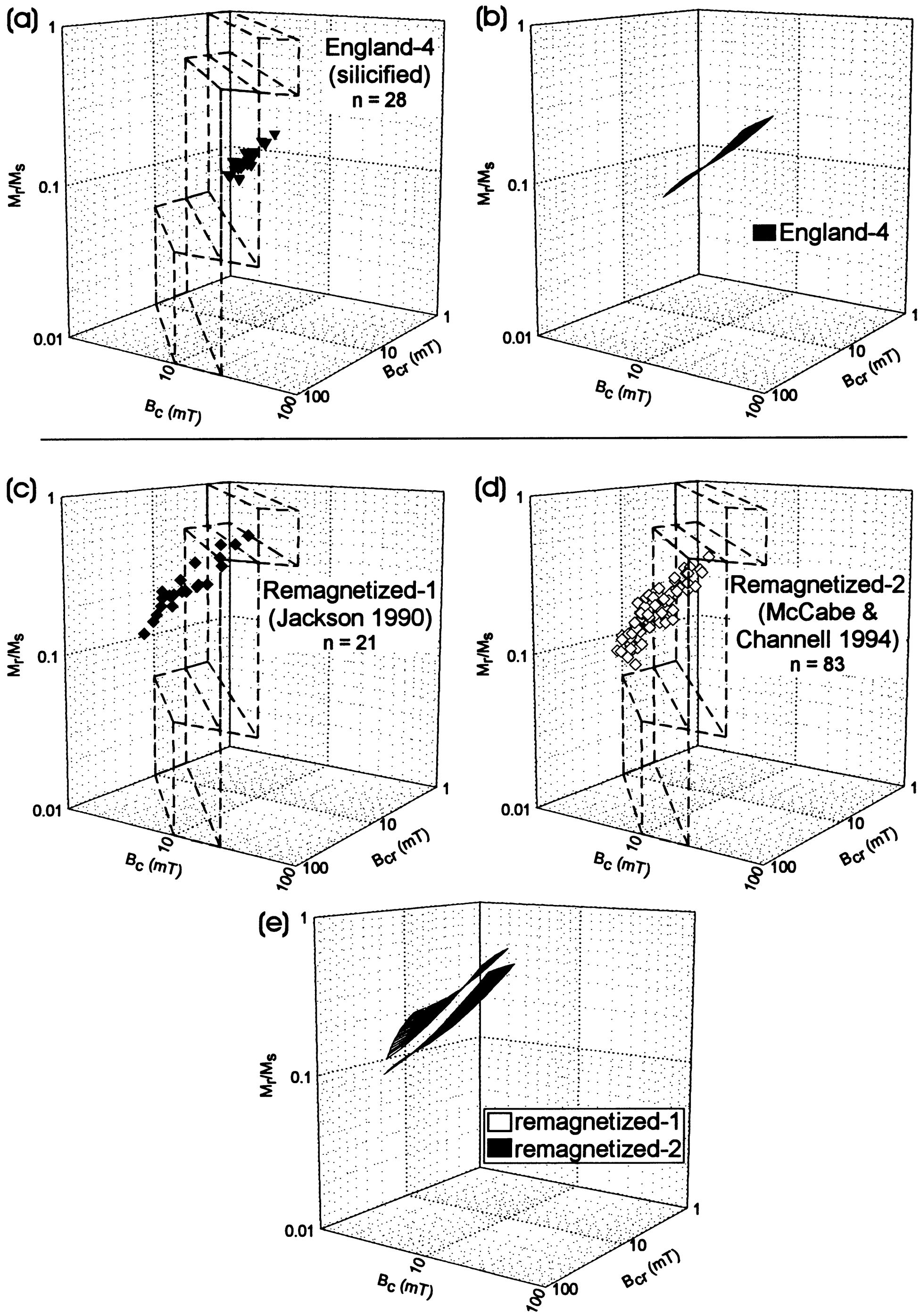

Figure 10. Silicified limestones from (a,b) Maher *et al.* (2000); chemically remagnetized limestones (c) Jackson (1990) and Jackson *et al.* (1993), and (d) McCabe & Channell (1994). (c) shows results of studies of the Kiaman chemical remagnetization event that affected limestones in the northeastern United States. They have the regression surfaces with the highest M_r/M_s values and moderate inclination and lie outside the traditionally defined PSD space because their B_c values are anomalously low. Although not remagnetized in the regionally significant sense of Jackson *et al.* (1990), silicified shelf limestones from England show superficially similar characteristics regarding the inclination and relatively high M_r/M_s value of their regression surface (compare b, e).

hysteresis regression surfaces is also progressive, confirming for a single depositional basin (Fig. 7) what we observe in our compilations from many sources (Figs 8 and 9). We suggest that the hysteresis parameters are primarily controlled by depositional environment. The offshore, deeper sediments accumulate slowly, typically a few millimetres per thousand years. Thus, atmospheric, extraterrestrial and organic influx of magnetite could represent a high proportion of the sediment. It is really unimportant whether biogenic magnetite is intracellular, from magnetotactic bacteria, or the more copious byproduct of iron-reducing bacteria (Moskowitz *et al.* 1989). The former is more likely but, in principle, it is possible to

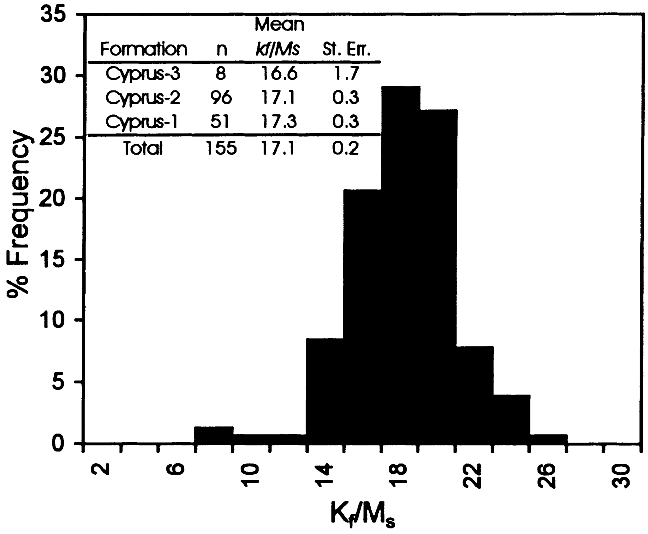

Figure 11. Jackson *et al.* (1993) and Moskowitz *et al.* (1988, 1989) showed that (K_f/M_s in μm A^{-1}) could be diagnostic for either chemically remagnetized limestones ($\sim$80 μm A^{-1}) or those bearing bacterial magnetite ($\leq$35 μm A^{-1}), whereas stable SD and larger grains have $\leq$8 μm A^{-1} and SP grains have $\sim$50 μm A^{-1}. We found the ratio to be less diagnostic in our study, generally indicating behaviour that could be compatible with any small SD grains of bacterial, volcanic or detrital origin. The Lefkara Formation (Cyprus-1) had the deepest depositional environment and the Nicosia Formation (Cyprus-3) had the shallowest.

distinguish between the two possibilities because magnetotactic bacteria produce magnetite in a restricted size range (Moskowitz *et al.* 1989). Iron-reducing bacteria produce a wider range of grain sizes, including much SP material and some large PSD grains. Moreover, the concatenation of SD magnetite grains in magnetotactic bacteria causes interactions that make magnetization more difficult than demagnetization (Cisowski 1981). However, this test may not always be decisive because fragile magnetosome should disrupt during compaction or diagenesis, and especially in the case of tectonic deformation.

In near-shore, shallower depositional environments, coarser magnetite should be more prevalent, for example imported with clastic clay minerals. This would explain the more common PSD response in this depositional environment. As well as changing proportions of biological versus physically derived magnetite in the different environments, one might expect several biological sources, for example different bacterial species, and chiton teeth. Of the 557 limestone samples studied, the PSD response is almost universal, with MD behaviour detected in only three samples from England-1, six samples from England-3, three samples from England-5 and one sample from Israel, and a complete absence of SD magnetite with the exception of one sample from Jackson's remagnetized suite.

Palaeomagnetists need criteria by which to identify remagnetized rocks which are unsuitable for palaeomagnetic studies (Jackson 1990; Jackson *et al.* 1992; McCabe & Channell 1994; Channell & McCabe 1994). The remagnetized limestones that we studied and reviewed are characterized by regression surfaces that are as steep as those for pelagic chalks, but displaced upwards above the conventional SD-PSD-MD sequence with high M_r/M_s intercepts (Figs 10c to e). Thus, we can be optimistic that remagnetized limestones can be identified and rejected on the basis of simple hysteresis measurements.

ACKNOWLEDGMENTS

We are particularly grateful to Mike Jackson for a very helpful and constructive review, particularly the suggestion to use logarithmic axes for M_r/M_s. J. Channell kindly provided the original data from Channell & McCabe (1994) and McCabe & Channell (1994). The work was funded by the Natural Sciences Engineering Research Council of Canada to Graham Borradaile.

REFERENCES

Banerjee, S.K. & Moskowitz, B.M., 1985. Ferrimagnetic properties of magnetite, in *Magnetite Biomineralization and Magnetoreception in Organisms: a New Biomagnetism,* pp. 17–41, eds Kirschvink, J.L., Jones, D.S. & Macfadden, B.F., Plenum Press, New York.

Bernouilli, D. & Jenkyns, H.C., 1974. Alpine, Mediterranean, and Central Atlantic Mesozoic facies in relation to early evolution of the Tethys, in *Modern and Ancient Geosynclinal Sedimentation,* eds Dott, R.H. & Shaver, R.H., *Soc. Econ. Paleontol. Min., Spec. Publ.,* **19,** 129–160.

Blakemore, R.P., 1975. Magnetotactic bacteria, *Science,* **190,** 377–379.

Borradaile, G.J., 1991. Remanent magnetism and ductile deformation in an experimentally deformed magnetite-bearing limestone, *Phys. Earth planet. Inter.,* **67,** 362–373.

Borradaile, G.J., 1992. Experimental deformation of two-component IRM in magnetite-bearing limestones: a model for the behavior of NRM during natural deformation, *Phys. Earth planet. Inter.,* **70,** 64–77.

Borradaile, G.J., 1994. Magnetic remanence in the Chalk of eastern England: an unusually resistant VRM?, *Geol. Mag.,* **131,** 593–608.

Borradaile, G.J., 1999. Viscous remanent magnetization of high thermal stability in limestones, in *Paleomagnetism and Diagenesis in Sediments,* eds Tarling, D.H. & Turner, P., *Geol. Soc. Lond., Spec. Publ.,* **151,** 27–42.

Borradaile, G.J. & Brann, M., 1997. Remagnetization dating of Roman and Mediaeval masonry, *J. archeol. Sci.,* **24,** 813–824.

Borradaile, G.J., Chow, N. & Werner, T., 1993. Magnetic hysteresis of limestones: Facies control?, *Phys. Earth planet. Inter.,* **76,** 241–252.

Chang, S.-B.R. & Kirschvink, J.L., 1989. Magnetofossils, the magnetization of sediments, and the evolution of magnetite biomineralization, *Ann. Rev. Earth planet. Sci.,* **17,** 169–195.

Channell, J.E.T. & McCabe, C., 1994. Comparison of magnetic hysteresis parameters of unremagnetized and remagnetized limestones, *J. geophys Res.,* **99,** 4613–4623.

Churnet, H.G., Misra, K.C. & Walker, K.R., 1982. Deposition and dolomitization of Upper Knox carbonate sediments, Copper Ridge district, East Tennessee, *Geol. Soc. Am. Bull.,* **93,** 76–86.

Cisowski, S., 1981. Interacting vs. non-interacting single-domain behaviour in natural and synthetic samples, *Phys. Earth planet. Inter.,* **26,** 77–83.

Day, R., Fuller, M.D. & Schmidt, V.A., 1977. Hysteresis properties of titanomagnetites: grain size and compositional dependence, *Phys. Earth planet. Inter.,* **13,** 260–267.

Dunlop, D.J. & Özdemir, Ö., 1997. *Rock Magnetism: Fundamentals and Frontiers, Cambridge Studies in Magnetism.* Cambridge University Press, Cambridge.

Earp, J.P., Magraw, D., Poole, E.G., L., D.H. & Whiteman, A.J., 1961. Geology of the country around Clitheroe and Nelson, *Mem. geol. Surv. England,* **9.**

Frankel, R.B., Blakemore, R.P., Torres de Araujo, F.F., Esquivel, D.M.S. & Danon, J., 1981. Magnetotactic bacteria at the geomagnetic equator, *Science,* **212,** 1269–1270.

Freeman, R., 1986. Magnetic mineralogy of pelagic limestones, *Geophys. J. R. astr. Soc.,* **85,** 433–452.

Gass, I.G., 1960. The geology and mineral resources of the Dhali Area, *Mem. Geol. Surv. Cyprus,* **4**.

Gass, I.G. & Cockbain, A.F., 1961. Notes on the occurrence of Gypsum in Cyprus, *Overseas Geol. Miner. Resour.,* **8,** 279–287.

Henshaw, P.C. & Merrill, R.T., 1980. Magnetic and chemical changes in marine sediments, *Rev. Geophys. Space Phys.,* **18,** 483–504.

Henson, F.R.S., Browne, R.V. & McGinty, J., 1949. A synopsis of the stratigraphy and geological history of Cyprus, *Q. J. geol. Soc. Lond.,* **105,** 1–41.

Jackson, M., 1990. Diagenetic sources of stable remanence in remagnetized Paleozoic cratonic carbonates: a rock magnetic study, *J. geophys. Res.,* **95,** 2753–2761.

Jackson, M., 1999. Measure for Measure: The beauty of magnetic units, *IRM Quarterly,* **9,** 1–2.

Jackson, M. & Sun, W.-W., 1992. The rock magnetic fingerprint of chemical remagnetization in midcontinental Paleozoic carbonates, *Geophys. Res. Lett.,* **19,** 781–784.

Jackson, M., Rochette, P., Fillion, G., Banerjee, S. & Marvin, J., 1993. Rock magnetism of remagnetized Paleozoic carbonates: Low-temperature behavior and susceptibility characteristics, *J. geophys. Res.,* **98** (B4), 6217–6225.

Jeans, C.V., 1973. The Market Weighton Structure: tectonics, sedimentation and diagenesis during the Cretaceous, *Proc. Yorkshire geol. Soc.,* **39,** 409–444.

Kay, M., 1968. Ordovician formations in northwestern New York, *Naturaliste Canadien,* **95,** 1373–1378.

Kirschvink, J.L., 1982. Paleomagnetic evidence for fossil biogenic magnetite in western Crete, *Earth planet. Sci. Lett.,* **59,** 388–392.

Kirschvink, J.L. & Lowenstam, H.A., 1979. Mineralization and magnetization of chiton teeth: Palaeomagnetic, sedimentologic, and biologic implications of organic magnetite, *Earth planet. Sci. Lett.,* **44,** 193–204.

Kirschvink, J.L., Maine, A.T. & Vali, H., 1997. Paleomagnetic evidence of a low-temperature origin of carbonate in the Martian meteorite ALH 84001, *Science,* **275,** 1629–1633.

Lagroix, F. & Borradaile, G.J., 2000. Tectonics of the circum-Troodos sedimentary cover of Cyprus, from magnetic and structural observations, *J. struct. Geol.,* in press.

Lowenstam, H.A., 1962. Magnetite in denticle capping in recent chitons (Polycophora), *Geol. Soc. Am. Bull.,* **73,** 435–438.

Lowrie, W. & Heller, F., 1982. Magnetic properties of marine limestones, *Rev. Geophys. Space Phys.,* **20,** 171–192.

Lu, G., McCabe, C., Hanor, J.S. & Ferrell, R.E., 1991. A genetic link between remagnetization and potassic metasomatism in the Devonian Onondaga Formation, Northern Appalachian Basin, *Geophys Res. Lett.,* **18,** 2047–2050.

McCabe, C. & Channell, J.E.T., 1994. Late Paleozoic remagnetization in limestones of the Craven Basin (northern England) and the rock magnetic fingerprint of remagnetized sedimentary carbonates, *J. geophys. Res.,* **99,** 4603–4612.

McCabe, C., Van der Voo, R. & Ballard, M.M., 1984. Late Paleozoic remagnetization of the Trenton Limestone, *Geophys. Res. Lett.,* **11,** 979–982.

Mackereth, F.J.H., 1971. On the variation in direction of the horizontal component of remanent magnetization in lake sediments, *Earth planet. Sci. Lett.,* **12,** 332–338.

Maher, L., Borradaile, G.J., Stewart, J.D. & O'Connor, M., 2000. Primary or secondary insertion of the Romanesque Frieze at Lincoln Cathedral, England? Magnetic considerations, *Archeometry,* in press.

Mantis, M., 1970. Upper Cretaceous-Tertiary Foraminiferal Zones in Cyprus, *Epithris,* **3,** 227–241.

Moskowitz, B.M., Frankel, R.B., Bazylinski, D.A., Jannasch, H.W. & Lovley, D.R., 1989. A comparison of magnetite particles produced anaerobically by magnetotactic and dissimilatory iron-reducing bacteria, *Geophys. Res. Lett.,* **16,** 665–668.

Moskowitz, B.M., Frankel, R.B., Flanders, P.J., Blakemore, R.P. & Schwartz, B.B., 1988. Magnetic properties of magnetotactic bacteria, *J. magn. Mater.,* **73,** 273–288.

Oliver, W.A., 1960. Coral faunas in the Onondaga limestone of New York, *US Geol. Surv. Prof. Pap.,* **100-B,** 172–174.

Wasilewski, P.J., 1973. Magnetic hysteresis in natural materials, *Earth planet. Sci. Lett.,* **20,** 67–72.